

# **SUPPLEMENTAL MATERIAL**

## **Data S1. Supplemental Methods**

### **Propagation pattern characterisation**

Propagation patterns described are identified using AcQTrack, an integrated platform within the AcQMap system. The propagation history map is first generated based on virtual dipole signals from each of approximately 3,500 vertices on the chamber surfaces and derived from biopotential signals recorded on 48 non-contact electrodes. This map allows visualisation of wavefronts over the atrial surface. AcQTrack evaluates the propagation of these wavefronts to identify specific patterns of activation. Every vertex of the chamber is continuously analysed during the display of the propagation history map thereby allowing real-time identification of regions of interest, which can be displayed as both a dynamic map (where each activation pattern is highlighted during playback of the propagation history) and a cumulative map, where a sliding scale allows adjustment to the display according to the frequency of each pattern detected at any localised site. Patterns of activation identified include focal firing (FF), localised irregular activation (LIA) and localised rotational activation (LRA), with the specific algorithm used for their detection described below. Wavefronts that do not meet these definitions (for example smooth planar wavefronts) are discounted.

#### **Focal firing (FF)**

- The focal activation algorithm determines whether an activation at a vertex came from a previous cardiac wavefront, or whether activation spontaneously started from the current activation. Focal activation is detected at a vertex if an activation is earlier than its neighbors' activation by at least 2-5 ms (default 3ms), and conduction spreads outward from the early activation.
- Activations are connected as a wavefront if the time difference between the two activation times would produce a conduction velocity greater than 0.05 m/s.

#### **Localised irregular activation (LIA)**

- The localised irregular activation algorithm computes the difference in angle between cardiac conduction entering and leaving a confined region, as illustrated in **Figure S1**. If the angle difference of conduction entering and leaving a confined region exceeds 90 degrees, localised irregular activation is detected in the region.
- An area of approximately 200-300 mm<sup>2</sup> is considered a confined region
- Wavefronts are considered to be passing through the region if the activation times differences between the border of the confined region and the central vertex would result in a conduction velocity between 0.3 m/s to 3.0 m/s.
- Activations are grouped into entering and leaving the region based on the activation time with comparison to the central vertex. A mean conduction vector entering the region and leaving the region are then computed. Angle difference between the vector entering and leaving the region are computed and if the difference exceeds 90 degrees, LIA is detected.

### **Localised rotational activation (LRA)**

- The localised rotational activation algorithm computes the degrees of conduction propagation around a central point by summing the angle differences of sequential conduction velocity vector directions around the central point, as illustrated in **Figure S2**. If the rotational angle of conduction vector changes exceeds 270 degrees, equating to total angle of propagation change of 360 degrees, rotation is detected at the central point. An area of approximately 200-300 mm<sup>2</sup> around the central point is considered.
- To ensure smooth propagation around the central point, an  $r^2$  of a linear fit of activation time to position around the central vertex must exceed 0.7.
- Conduction velocity vector directions changes cannot exceed 45 degrees per position change around the vertex

- Activation time difference around the central obstacle must be greater than 50ms.

## **Propagation pattern quantification**

Quantification of these propagation patterns is required to enable comparisons. Both global measures of activation patterns across the chamber as well as methods to localise specific regions with highly repetitive activation were needed. Occurrences of these activation patterns in any given recording are often distributed widely across the chamber at low frequency with clustering of patterns at higher frequency. However, the specific frequency threshold that differentiates localised regions of most repetitive activation is highly variable between patients and maps. Whilst in one recording of a fixed duration a specified frequency threshold may be suitable, in another recording the frequency across the whole chamber may be above this threshold (as a result of different properties of AF propagation between patients/recordings) meaning that no activation occurrences are excluded and the region with the most repetitive patterns therefore not differentiated. A method that considers these observations was required allowing comparison of the statistical properties of each map obtained with the requirement to:

1. Be able to quantify global chamber occurrences to quantify “substrate properties”
2. Able to exclude infrequent occurrences that may represent false positive detections or isolated findings unlikely to be mechanistically significant
3. Identify localised regions with the most repetitively occurring patterns that may be targeted by ablation
4. Provide output according to the number of occurrences of each pattern, the proportion of time the patterns were present, and the proportion of the chamber surface area affected

A custom designed programme was developed with the aim of meeting these requirements. The process is outlined in **Figure S3**. Initially, all AcQTrack data is exported to

create a static map quantifying every pattern occurrence at each vertex of the chamber anatomy for the entire recording duration (**Figure S3A**). Each single occurrence of an activation pattern identified by AcQTrack is represented as a patch of the chamber surface that occupies all vertices within the specific confined zone (of 200-300mm<sup>2</sup>) at which the activation pattern is detected by AcQTrack (as outlined above) and for the specific period of time that the pattern remains (**Figure S3B**). The number of these unique patches equates to the number of occurrences of the specified propagation pattern (**Figure S3C**). When taken over the duration of the recording, the proportion of time in which activation patterns are detected on the chamber surface represents the time parameter (**Figure S3C**). Similarly, the proportion of the chamber in which an occurrence is detected represents the surface area affected (**Figure S3D**). Where occurrences overlapped in both space and time, potentially representing a pivot point that drifts across a region rather than remaining at a single anatomical vertex these were counted as a single occurrence (as seen in **Figure S3C**). In addition, a 5ms inclusion tolerance is included where occurrences are detected separately but within the same location less than 5ms apart. This is to ensure that an occurrence is not double counted when a short period is seen during which the AcQTrack parameters are not met but the time duration is too short to account for a separate wavefront activating that region. When this is applied to the threshold regions (described below) to quantify pattern occurrences within these zones, only patches where the centre falls within the specified zone is counted rather than any patch that purely overlaps that region.

Cut off thresholds are then applied to exclude outlying data and identify the localised regions with the most repetitive pattern occurrences. The number of occurrences in each region and the proportion of time that they are present are known. These factors are therefore used to determine the threshold. The initial static map displays all occurrences with no cut off applied (in **Figure 2** in the main paper; zero on the x axis i.e. every occurrence is counted). The percentage of the recording time with the relevant pattern is shown on the Y axis. As the cut off is increased along the X axis, i.e. only regions with increasing numbers of

occurrences are included, the proportion of time these are present decreases. A standardised cut off for the minimum absolute number of occurrences in any region does not allow for a relative correction for the varying total numbers between patients. For example where very high numbers are detected in one map with a minimum of five occurrences in any single region, then a cut off of 4 would not exclude any outlying data, compared to another map where very few detections were seen and the same cut off disproportionately excludes important data. Furthermore, an absolute cut off does not take into account the recording duration analysed. Our approach applies a threshold relative to the total time pattern occurrences are present, as illustrated in figure 2. Thresholds can then be applied that result in an exclusion of occurrences resulting in a reduction in the percentage of time that LIA is present. The highest threshold identifies the region with only the most repetitive activation pattern occurrences.

For the example used in figure 2, a colour coded representation of the number of LIA occurrences for each of the (approximately) 3500 vertices on the left atrial geometry is provided. Cut-offs were then used to eliminate the low frequency vertices, which is also those in which LIA activity was present for a relatively small proportion of the total percentage time any LIA activity was present at any part of the whole chamber. The X axis has all 3500 vertices grouped by the minimum number of individual LIA occurrences seen at that vertex during that 5-second recording. The Y axis represents the percentage of time that at least 1 of the 3500 vertices displayed LIA activity during the 5-second segment. In this example the chart indicates that for 91% of the time, any vertex which showed 1 or more LIA occurrences during the recording was exhibiting that activity (thus, for 9% of the 5 second recording there was no LIA activity at any site). To eliminate those vertices which only very infrequently displayed occurrences, a 5% cut off is introduced. This is a relative 5% of the overall percentage time that one or more occurrences were present during the recording and thus the threshold moves down from 91% to 86.5% of the overall percentage time. This has the impact of excluding those low frequency vertices which contributed very

little to the total time that one or more LIA were present, eliminating the red and most of the orange and yellow colours.

When the threshold is increased to a 10% cut-off (and drops to a total percentage time of 81.9%), this has the effect of excluding all of the vertices which had 5 or fewer LIA occurrences, eliminating more yellow and green colour-coded areas. Finally, a 20% cut off moves the threshold of percentage time LIA were present at any point on the whole chamber from 91% down to 72.8% and in doing so in this patient's recording excludes all of those vertices which displayed 8 separate LIA occurrences or fewer and the colour coding on the map is focused in on the green and dark blue areas.

What can be demonstrated in the bar chart is that the small area in purple, surrounded by dark blue, that demonstrated the most individual LIA occurrences, occupied less than 10% of the recording segment time, i.e. the 21 individual LIA occurrences occurring in those vertices had a cumulative time of less than 0.5 of a second. This is because LIA activity is a depolarisation phenomenon and will not be present during repolarisation, which takes up the majority of the cycle length. The very nature of slow, pivoting and stuttering propagation may also lead to one very disorganised wavefront being counted as multiple LIA occurrences, hence the need to incorporate percentage time as a modifier. If it was desirable to show all vertices which showed 5 or more LIA occurrences during the 5-second segment, the threshold would need to be decreased to less than 5% (i.e. no cut-off) and a much larger number of vertices would be shown across a wider colour range and percentage time of the 5 second segment

Further impetus for this approach is that there may not be a fixed relationship between the frequency of pattern occurrences and the duration that the patterns are present. Fewer occurrences may persist for longer (e.g. multiple rotations of LRA) in one recording whilst a higher frequency in another recording (e.g. short-lived pivoting LIA) may last for shorter durations. This is illustrated in figure S4. In scenarios with a high frequency of pattern occurrences and a high degree of clustering a threshold method of either a fixed percentage

of occurrences or the dynamic thresholding method explained above produce similar results (S4A). However, in examples with a less clearly delineated cluster or a lower frequency of occurrences, a fixed percentage method resulted in exclusion of areas with a high number of occurrences that persist for a longer duration and therefore may be mechanistically important (S4B, C).

### Supplemental Figures

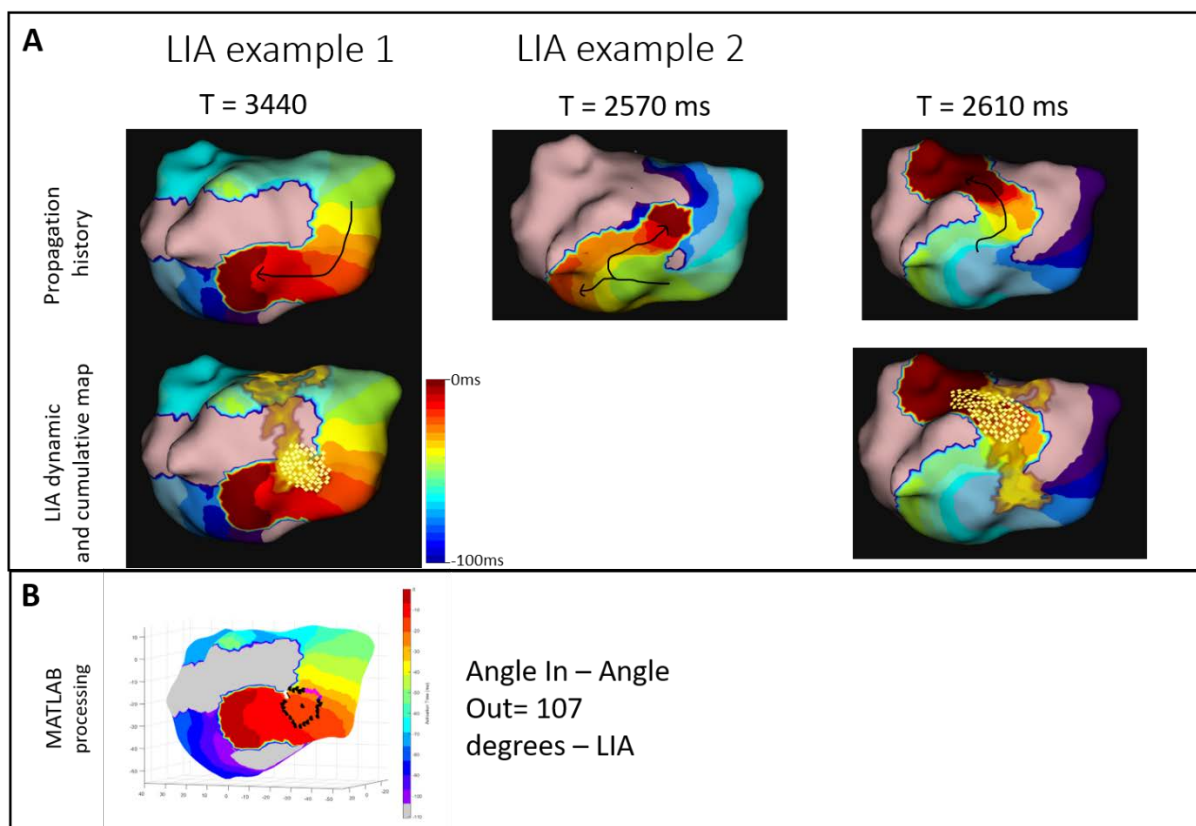


**Figure S1** Examples of patterns characterised as LIA are shown in A. Top row shows static images of a propagation history map taken at 3 time points with the row below including the dynamic view of LIA detection (yellow dots) and the cumulative map (yellow patch overlay) highlighting a region over the posterior wall where a frequency of LIA above a specified (user defined) threshold was detected. Panel B illustrates the computational processing that results in LIA classification for example 1. Red denotes the leading edge of the wavefront and purple the trailing edge. The time difference used for this display can be adjusted manually (here it is set to 100ms).



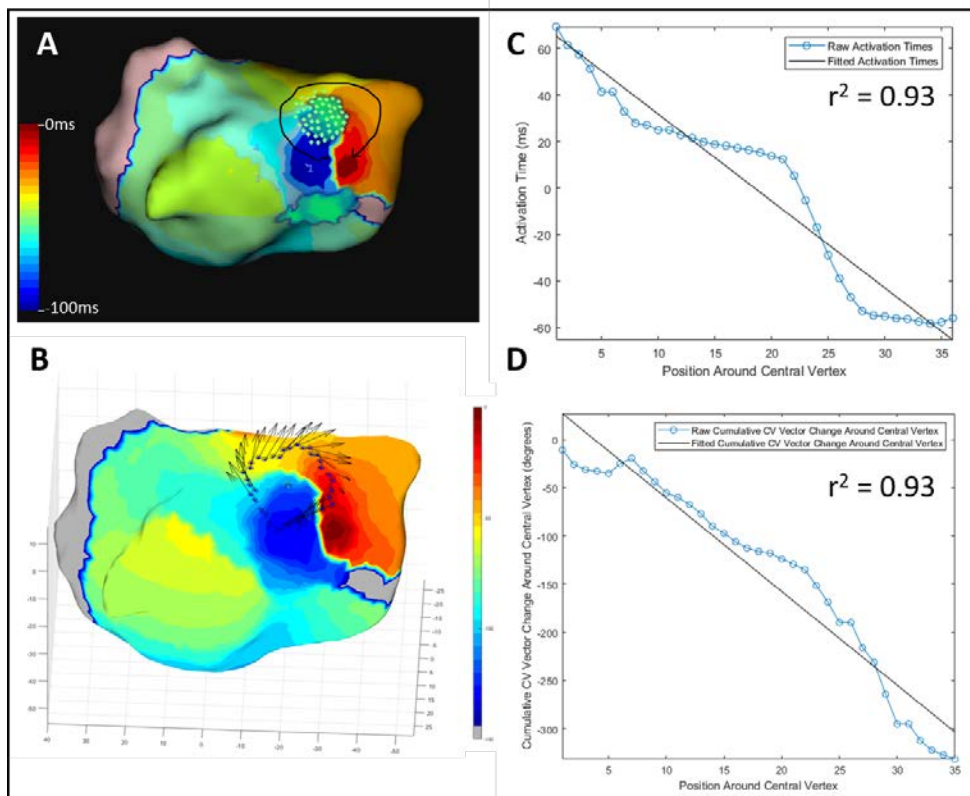


**Figure S2** (A) shows a static propagation history map including the dynamic view of LRA detection (green dots) and the cumulative map (green patch overlay) highlighting a region where a frequency of LRA above a specified (user defined) threshold was detected. (B) illustrates the processing and where activation times (C) and vectors (D) are plotted at points around a central vertex within the algorithm. As in figure S1, red denotes the leading edge of the wavefront and purple the trailing edge with the time difference set to 100ms.

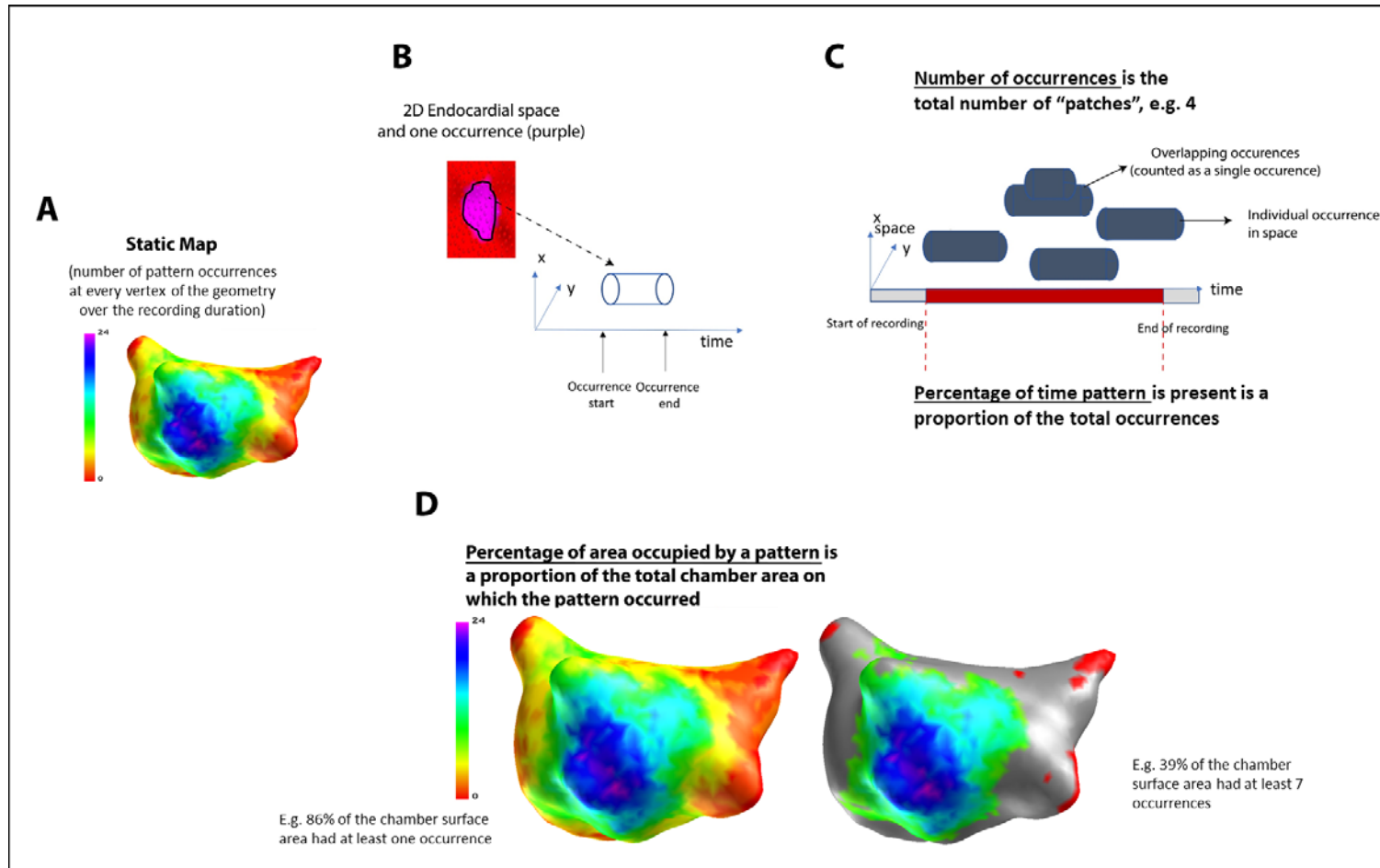


**Figure S3** Method for AcQTrack pattern quantification. A static map is generated (A) demonstrating all pattern occurrences. Each occurrence is identified in space as the confined zone on the endocardial surface at which the activation pattern is detected by AcQTrack (in B shown as a purple patch on the red chamber surface and represented for illustrative purposes by a single cone) for the duration of time that the pattern remains (B) allowing calculation of the total number of occurrences and the percentage time they are present (C), as well as the proportion of the chamber surface area affected (D).

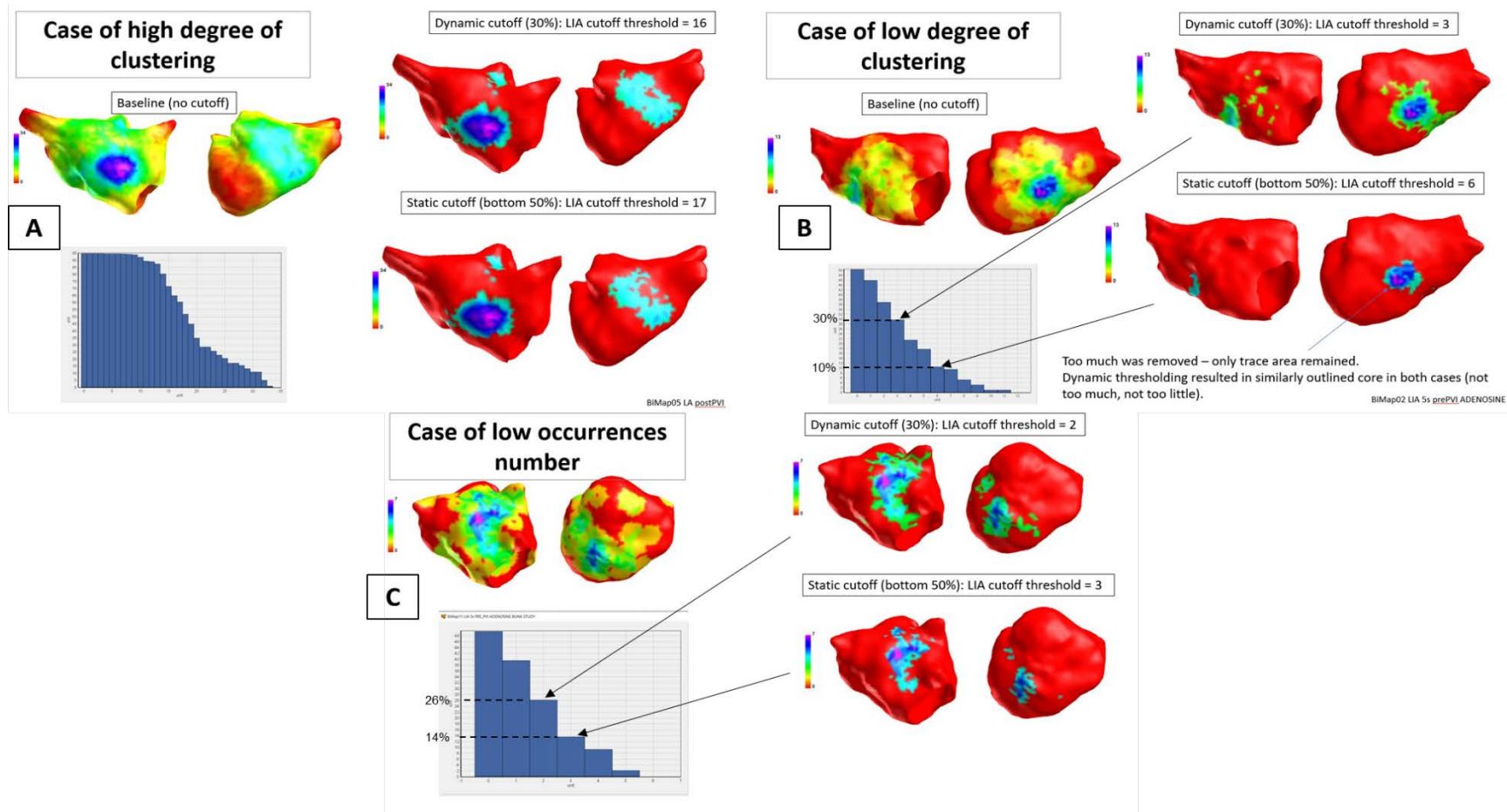


**Figure S4** In a case with a high frequency of occurrences and high degree of clustering both a percentage frequency and a dynamic threshold approach produce similar results (A). However, where there is less clear clustering (B) a fixed percentage approach excludes regions where patterns occur for a significant duration i.e. exclusion is too high therefore potentially excluding areas of importance. This may also be the case in an example with a low frequency of patterns that last for a relatively longer period of time (C).

## Supplemental Tables

Variable	Cut off (%)	Pre-PVI				Post-PVI				Post non-PVI ablation			
		Baseline (SD)	Adenosine (SD)	Difference (95% CI)	p value	Baseline (SD)	Adenosine (SD)	Difference (95% CI)	p value	Baseline (SD)	Adenosine (SD)	Difference (95% CI)	p value
LRA number	0	18±8.5	22.5±8.5	4.8 (-2.9 – 12.0)	0.2044	15.9±8.0	25.6±12.4	9.7 (2.0 – 17.5)	0.0173	14.2±5.8	24.0±6.3	9.8 (5.5 – 14.1)	0.0007
	5	12.9±6.7	17.1±7.3	4.2 (-1.5 – 9.9)	0.1360	11.5±7.0	20.1±10.1	8.6 (1.4 – 15.8)	0.0230	9.1±5.2	17.8±5.2	7.9 (4.4 – 12.9)	0.0016
	10	11.9±6.9	16.9±7.2	5.0 (-0.6 – 10.6)	0.0749	10.7±6.6	18.9±9.8	8.2 (1.5 – 14.8)	0.0203	9.1±5.2	17.6±5.2	8.5 (3.9 – 13.0)	0.0027
	20	8.2±6.3	13.4±4.4	5.5 (0.5 – 9.9)	0.0345	9.0±5.4	14.5±8.4	5.5 (-0.6 – 11.6)	0.0720	7.8±3.8	14.1±5.3	6.3 (1.9 – 10.8)	0.0116
	30	7.3±5.0	10.9±3.9	3.6 (-0.1 – 7.4)	0.0551	6.5±4.0	11.5±6.1	5.0 (1.3 – 8.6)	0.0118	6.9±3.4	12.3±4.3	5.4 (1.3 – 9.6)	0.0156
	40	6.5±4.4	9.3±3.3	2.8 (-0.6 – 6.0)	0.0935	4.8±2.9	10.7±5.5	5.9 (2.2 – 9.5)	0.0040	5.3±2.1	10.2±3.5	4.9 (2.9 – 6.9)	0.0005
LRA time	0	34.2±14.2	40.9±14.3	6.7 (-5.6 – 18.9)	0.2537	27.8±9.7	46.3±19.4	18.5 (6.5 – 30.3)	0.0050	27.5±11.9	41.3±8.7	13.8 (4.7 – 22.8)	0.0079
	5	28.8±13.0	34.4±13.3	5.6 (-5.3 – 16.6)	0.2810	23.4±10.1	41.3±17.9	17.9 (6.2 – 29.4)	0.0053	20.9±11.6	34.7±8.3	13.8 (5.4 – 22.3)	0.0054
	10	27.4±13.5	34.0±13.0	6.6 (-4.1 – 17.3)	0.2011	22.5±9.4	39.3±17.6	16.8 (6.0 – 27.6)	0.0048	20.9±11.6	34.3±8.2	13.4 (4.4 – 22.3)	0.0090
	20	19.8±12.5	28.8±10.5	9.0 (-2.0 – 20.0)	0.0991	19.9±9.6	32.4±16.3	12.5 (1.4 – 23.6)	0.0301	18.9±9.8	28.2±6.7	9.3 (1.2 – 17.5)	0.0297
	30	18.6±10.9	24.6±8.7	6.0 (-3.1 – 14.9)	0.1722	15.7±7.8	26.4±13.4	10.7 (3.4 – 17.9)	0.0069	17.0±9.0	25.2±6.5	8.2 (0.6 – 15.7)	0.0381
	40	17.5±10.1	21.8±7.7	4.3 (-3.6 – 12.3)	0.2491	11.9±6.0	24.7±11.9	12.8 (5.0 – 20.6)	0.0033	13.1±5.4	21.7±7.1	8.6 (4.5 – 12.8)	0.0014
LRA SA	0	25.6±8.7	28.0±10.2	2.4 (-4.9 – 9.7)	0.4776	21.1±8.0	30.9±12.2	9.8 (1.7 – 17.8)	0.0213	20.2±8.1	29.5±6.7	9.3 (5.6 – 13.0)	<0.0005
	5	16.0±6.9	15.8±7.6	-0.2 (-5.6 – 5.3)	0.9414	12.1±6.3	16.8±7.4	4.7 (-1.8 – 11.2)	0.1407	9.5±4.8	14.9±4.3	5.4 (3.3 – 7.4)	<0.0005
	10	13.5±6.2	15.5±7.7	2.0 (-3.2 – 7.8)	0.4105	10.3±4.9	14.4±6.6	4.1 (-0.9 – 9.2)	0.0990	9.5±4.8	14.3±4.1	4.8 (2.0 – 7.5)	0.0041
	20	7.7±4.1	10.9±4.1	3.2 (0.3 – 6.2)	0.0342	7.9±3.3	9.6±4.8	1.6 (-2.2 – 5.6)	0.3788	7.5±2.7	10.1±3.3	2.6 (0.6 – 4.5)	0.0162
	30	6.8±2.5	8.6±4.7	1.8 (-0.9 – 4.7)	0.1633	5.1±2.3	6.9±3.5	1.8 (-0.2 – 3.8)	0.0733	6.4±2.8	7.8±2.3	1.4 (-0.6 – 3.6)	0.1312
	40	5.8±1.9	6.8±3.1	1.0 (-0.6 – 2.6)	0.1843	3.7±2.0	6.1±3.1	2.4 (0.1 – 2.6)	0.0417	5.0±2.3	6.1±2.3	1.1 (-0.3 – 2.6)	0.1097

**Table S1.** Impact of adenosine of LRA frequency, duration and surface area, pre-pulmonary vein isolation, post-pulmonary vein isolation and following non-pulmonary vein ablation. LRA: Localised rotational activation; PVI: pulmonary vein isolation; SA: surface area.

Variable	Cut off (%)	Group	n	Mean	Standard deviation	p-value	95 % Confidence interval
LRA number	0	DCCV	16	16.9	7.9	0.0760	-0.8 – 13.8
		Sinus with ablation	6	10.3	5.0		
LRA percent time	0	DCCV	16	31.8	13.1	0.0970	-2.1 – 23.1
		Sinus with ablation	6	21.3	10.9		
LRA percent SA	0	DCCV	16	23.7	8.4	0.0380	0.5 – 16.6
		Sinus with ablation	6	15.1	6.8		
LRA number	5	DCCV	16	12.3	6.0	0.0590	-0.2 – 11.2
		Sinus with ablation	6	6.8	4.8		
LRA percent time	5	DCCV	16	26.8	12.2	0.0760	-1.2 – 22.1
		Sinus with ablation	6	16.3	10.0		
LRA percent SA	5	DCCV	16	14.6	7.0	0.0490	0.0 – 13.1
		Sinus with ablation	6	8.0	5.0		
LRA number	10	DCCV	16	11.1	5.8	0.1280	-1.3 – 9.8
		Sinus with ablation	6	6.8	4.8		
LRA percent time	10	DCCV	16	25.2	12.2	0.1270	-2.8 – 20.6
		Sinus with ablation	6	16.3	10.0		
LRA percent SA	10	DCCV	16	11.7	5.5	0.1690	-1.7 – 9.1
		Sinus with ablation	6	8.0	5.0		
LRA number	20	DCCV	16	9.0	5.2	0.0270	0.7 – 10.0
		Sinus with ablation	6	3.7	2.3		
LRA percent time	20	DCCV	16	20.8	10.8	0.0380	0.6 – 20.5
		Sinus with ablation	6	10.3	6.5		
LRA percent SA	20	DCCV	16	8.3	3.3	0.0080	1.3 – 7.5
		Sinus with ablation	6	3.9	2.3		
LRA number	30	DCCV	16	7.1	4.4	0.0780	-0.4 – 7.6
		Sinus with ablation	6	3.5	2.6		
LRA percent time	30	DCCV	16	17.4	9.7	0.0940	-1.4 – 16.8
		Sinus with ablation	6	9.8	7.3		
LRA percent SA	30	DCCV	16	6.1	2.5	0.0450	0.1 – 5.1
		Sinus with ablation	6	3.5	2.7		
LRA number	40	DCCV	16	6.1	4.1	0.1410	-1.0 – 6.6
		Sinus with ablation	6	3.3	2.5		
LRA percent time	40	DCCV	16	15.4	9.8	0.1740	-3.0 – 15.2
		Sinus with ablation	6	9.2	6.8		
LRA percent SA	40	DCCV	16	5.0	2.2	0.1220	-0.5 – 4.2
		Sinus with ablation	6	3.2	2.7		

**Table S2.** Difference in localised rotation activation frequency, duration and surface area at baseline according to acute procedural outcome.

Variable	Cut off (%)	Group	n	Mean	Standard deviation	p-value	95 % Confidence interval
LRA number	0	DCCV	16	22.7	9.1	0.738	-7.8 – 10.9
		Sinus with ablation	6	21.2	10.1		
LRA percent time	0	DCCV	16	40.7	14.5	0.971	-15.3 – 15.9
		Sinus with ablation	6	40.5	18.5		
LRA percent SA	0	DCCV	16	27.4	8.9	0.986	-10.5 – 10.3
		Sinus with ablation	6	27.5	14.1		
LRA number	5	DCCV	16	17.5	8.0	0.731	-6.6 – 9.3
		Sinus with ablation	6	16.2	7.9		
LRA percent time	5	DCCV	16	34.8	13.8	0.988	-14.3 – 14.5
		Sinus with ablation	6	34.7	16.2		
LRA percent SA	5	DCCV	16	15.1	6.0	0.943	-6.9 – 7.4
		Sinus with ablation	6	14.9	9.9		
LRA number	10	DCCV	16	16.9	7.6	0.715	-6.4 – 9.1
		Sinus with ablation	6	15.5	8.2		
LRA percent time	10	DCCV	16	34.0	13.7	0.998	-14.5 – 14.5
		Sinus with ablation	6	33.9	16.7		
LRA percent SA	10	DCCV	16	14.0	5.6	0.897	-7.6 – 6.7
		Sinus with ablation	6	14.4	10.3		
LRA number	20	DCCV	16	13.4	6.3	0.772	-5.3 – 7.1
		Sinus with ablation	6	12.5	5.8		
LRA percent time	20	DCCV	16	27.9	12.5	0.795	-14.4 – 11.2
		Sinus with ablation	6	29.6	13.7		
LRA percent SA	20	DCCV	16	10.1	4.5	0.941	-4.6 – 4.9
		Sinus with ablation	6	9.9	5.4		
LRA number	30	DCCV	16	11.2	4.9	0.388	-2.8 – 6.8
		Sinus with ablation	6	9.2	4.4		
LRA percent time	30	DCCV	16	23.2	10.0	0.88	-11.1 – 9.6
		Sinus with ablation	6	23.9	11.5		
LRA percent SA	30	DCCV	16	8.0	4.1	0.324	-2.2 – 6.2
		Sinus with ablation	6	6.0	4.4		
LRA number	40	DCCV	16	10.3	4.6	0.238	-1.9 – 7.2
		Sinus with ablation	6	7.7	4.4		
LRA percent time	40	DCCV	16	21.8	9.6	0.767	-8.6 – 11.5
		Sinus with ablation	6	20.3	11.3		
LRA percent SA	40	DCCV	16	7.0	3.0	0.126	-0.7 – 5.4
		Sinus with ablation	6	4.7	3.1		

**Table S3.** Difference in localised rotational activation frequency, duration and surface area following adenosine according to acute procedural outcome.